

CR-66065

DEVELOPMENT OF AN ORBIT DETERMINATION PROGRAM
TO REGRESS FOR LUNAR POTENTIAL CONSTANTS

By F. J. Lombard

GPO PRICE \$ _____
CFSTI PRICE(S) \$ _____
Hard copy (HC) \$ 2.00
Microfiche (MF) 1.50

653 July 65

Prepared under Contract No. NAS1-4605-3 by
TRW Systems
One Space Park, Redondo Beach, California

for

NATIONAL AERONAUTICS AND SPACE ADMINISTRATION

N 66 25553

FACILITY FORM 602

(ACCESSION NUMBER) 49 (THRU) 1
(PAGES) CR-66065 (CODE) 30
(NASA CR OR TMX OR AD NUMBER) (CATEGORY)

DEVELOPMENT OF AN ORBIT DETERMINATION PROGRAM
TO REGRESS FOR LUNAR POTENTIAL CONSTANTS

By F. J. Lombard

Prepared under Contract No. NAS1-4605-3 by
TRW Systems
One Space Park, Redondo Beach, California

for

NATIONAL AERONAUTICS AND SPACE ADMINISTRATION

ABSTRACT

This report describes the modifications made to the TRW Systems Orbit Determination Program in order to provide the capability of regressing for lunar potential constants. A mathematical explanation of the modifications is given together with a flow diagram and four test cases.

CONTENTS

	<u>Page</u>
1. SUMMARY	1
2. INTRODUCTION.	2
3. MATHEMATICAL FORMULATION.	4
3.1 Equations of Motion.	4
3.2 Variational Equations	8
3.3 Transformations from GPERT to TRAJ	16
4. TEST CASES.	18
4.1 Lunar Potential Model.	18
4.2 Description of Test Case	19
4.3 Running Time	20
5. CONCLUSIONS	29
6. NEW TECHNOLOGY.	29
APPENDIX I	31
APPENDIX II.	33
REFERENCES	39

ILLUSTRATION

	<u>Page</u>
1. Coordinate Transformations in the Integration of the Perturbative Accelerations	17

TABLES

I. Lunar Constants	18
II. Trajectory Description	19
III. Radar Stations	20
IV. Results Case A	22
V. Results Case B	24
VI. Results Case C	26
VII. Results Case D	28

SYMBOLS

A	matrix of partial derivatives of observations with respect to the state vector
a_f, a_g, a_h	accelerations in the selenographic system
C_{mm}, S_{mm}	sectoral harmonics
C_{nm}, S_{nm}	tesseral harmonics
E	expectation value
J_n	zonal harmonics
N_1	degree of highest zonal harmonic
N_2	degree of highest sectoral harmonic
N_3	degree of highest tesseral harmonic
n	vector of random noise
r	distance to vehicle from force center
U	gravitational potential function
W	weighting matrix
\hat{x}, \hat{x}	differential correction vector
x_t, \dot{x}_t	position and velocity components of the state vector
y	vector of residuals
z	vector of observations
α	right ascension of vehicle
γ_A	state vector at epoch
ϕ	selenographic longitude
μ	GM, mass of moon (or earth) times gravitational constant
σ	standard deviation

DEVELOPMENT OF AN ORBIT DETERMINATION PROGRAM
TO REGRESS FOR LUNAR POTENTIAL CONSTANTS

By F. J. Lombard
TRW Systems

1. SUMMARY

The TRW Orbit Determination Program has been modified to regress for lunar constants in a moon centered coordinate system using earth based observations. The program has the capability to solve for an arbitrary number of lunar potential constants as well as the usual six orbital parameters; station location errors and station observational biases may also be included. As many as 30 unknowns may be regressed for at one time.

The following procedure was followed in program checkout:

- a) Noised observations were generated from a trajectory integrated by using Goudas' lunar constants (see reference 1).
- b) A differential correction was then attempted using an initial estimate of the trajectory in which some or all of the lunar constants were perturbed ($\pm 3\sigma$) from their nominal (Goudas) values.
- c) Subsequent iterations of the tracking program were then examined to see if the nominal values of the lunar constants were recovered.

The first two cases involved about 10 hours of tracking on two different trajectories, with the solution vector including 12 lunar potential constants, i.e., the μ term of the moon plus the 11 potential constants of Goudas' model. The recovered values for the constants were found to be consistent with the covariance matrix describing their uncertainties.

The second two cases involved a single trajectory. In one case, 11 constants were perturbed and 7 were included in the solution vector; in the other case 11 were perturbed and the solution vector contained 9. Data arcs of

9-1/2 and 20 hours were used. The recovered values were not consistent with the covariance matrix, particularly in the case where only 7 constants were solved for, with errors sometimes many orders of magnitude larger than the respective standard deviation.

2. INTRODUCTION

The method used by the TRW Orbit Determination Program (AT85) for recovering lunar potential constants is termed the "direct" method. An alternative approach called the "long-period" method may also be used. This second method will be described later.

Suppose a trajectory is completely determined by a state vector γ_A ($n \times 1$) at a reference time (denoted as epoch), and further, suppose that a set of observations z ($m \times 1$) have been taken. In general, then

$$z = f(\gamma_A) + n$$

where n ($m \times 1$) is a vector of zero mean random noise. Thus taking the first-order terms of the Taylor expansion of f about an initial guess γ_0

$$z = z_0 + A(\gamma_A - \gamma_0) + n$$

where

$$z_0 = f(\gamma_0)$$

and

$$a_{ij} = \frac{\partial z_i}{\partial \gamma_j}$$

where a_{ij} is the element of the i^{th} row and j^{th} column. A component of the state

vector γ_i may be, e.g., the six orbital parameters, various lunar constants, radar biases, or station location errors. Let y ($m \times 1$) = $z - z_0$ be a vector of residuals, and x ($n \times 1$) = $\gamma_A - \gamma_0$ be the vector, known as the differential correction, to the initial guess γ_0 .

$$y = A x + n$$

The problem is then to determine an estimate of x which when added to γ_0 will yield an estimate of γ_A .

The AT85 program finds a value of x , calls it \hat{x} , which minimizes the product $(y - Ax)^T (y - Ax)$. It can be shown that the value of \hat{x} which does this is given by

$$\hat{x} = (A^T W A)^{-1} A^T W y$$

The matrix W ($m \times m$) is used to weight each individual observation. It is usually taken as a diagonal matrix with $W_{ii} = 1/\sigma_i^2$. The noise associated with the i^{th} observation is σ_i . The assumption is that there is no correlation between observations.

In addition, it can be shown that the covariance matrix associated with \hat{x} is given by

$$E (x - \hat{x}) (x - \hat{x})^T = (A^T W A)^{-1}$$

The A matrix, $a_{ij} = \partial z_i / \partial \gamma_j$ is calculated internally by the chain rule

$$A = \begin{pmatrix} \partial z \\ \partial \gamma \end{pmatrix}_{m \times n} = \begin{pmatrix} \partial z \\ \partial \alpha \end{pmatrix}_{m \times 6} \begin{pmatrix} \partial \alpha \\ \partial \gamma \end{pmatrix}_{6 \times n}$$

where α_i ($i = 1, 2, \dots, 6$) are the three components of position and velocity.

The matrix $\partial z/\partial \alpha$ is computed by explicit formulas, while the elements of the $\partial \alpha/\partial \gamma$ matrix are obtained by integrating the variational equations. A detailed account of their computation is given in section 3.2.

The long period method involves making a number of six-dimensional fits with nonoverlapping data arcs, assuming Keplerian motion. The sets of orbital elements, so called "mean elements," are then treated as observations. The observations are weighted by the inverse of the diagonal element of the covariance matrix $(A^T W A)^{-1}$, obtained in the 6 x 6 fit. Zero correlation is assumed in formulating the new weighting matrix. The partial derivatives come from solution of the equations of motion retaining only long-period and secular variations. Thus all the information is available to calculate A and z. The best estimate of the state \hat{x} can then be obtained by the previously described "direct" method.

3. MATHEMATICAL FORMULATION

3.1 Equations of Motion

Accelerations acting on the spacecraft are divided into those arising from the two-body portion of the central-body gravitational potential, and those resulting from the fact that the central body is not a homogeneous sphere. One function of the gravitational potential subroutine (GPRT) is to compute these perturbative accelerations. The interpretation of the GPRT equations is the same for both earth and moon. The expressions set forth here are for perturbative potential and accelerations; that is, the $-\mu/r$ term of the potential and the corresponding inverse square law accelerations are omitted.

Components of the perturbative acceleration are most easily expressed in a local rectangular coordinate system (f, g, h), with h along the outward geocentric vertical, f directed south, and g east. These are then transformed to an earth (or moon) centered system as will be explained later.

The potential function can be written as:

$$U = \mu \left[\sum_{n=2}^{N_1} r^{-n-1} J_n P_n(\sin \phi) - \sum_{n=2}^{N_2} r^{-n-1} \sum_{m=1}^{N_3} (C_{nm} \cos m\lambda + S_{nm} \sin m\lambda) P_n^m(\sin \phi) \right]$$

where

- r = distance from center of body
- ϕ = selenographic latitude
- λ = selenographic longitude
- μ = GM, mass of moon (or earth) times gravitational constant
- N_1 = degree of highest zonal harmonic
- N_2 = degree of highest sectorial harmonic
- N_3 = degree of highest tesseral harmonic

The accelerations are found by taking the gradient of the potential function; thus

$$a_f = \frac{1}{\mu r} \frac{\partial U}{\partial \phi}$$

$$a_g = - \frac{1}{\mu r \cos \phi} \frac{\partial U}{\partial \lambda}$$

$$a_h = - \frac{1}{\mu} \frac{\partial U}{\partial r}$$

where λ and ϕ are the geographic (or selenographic) longitude and latitude, respectively.

Carrying out this differentiation of the recursive potential function yields the acceleration as follows:

$$\begin{aligned}
 a_f &= \cos \phi \sum_{n=2}^{N1} \left(J_n r^{-n-2} \right) \rho'_n \\
 &+ \sum_{m=2}^{N2} m r^{-m-2} \sin \phi \left(\sec \phi \rho_m^m \right) (C_{mm} \cos m\lambda + S_{mm} \sin m\lambda) \\
 &- \sum_{m=1}^{N3} \sum_{n=m+1}^{N3} r^{-n-2} \left(\cos \phi \rho_n^{m'} \right) (C_{nm} \cos m\lambda + S_{nm} \sin m\lambda) \\
 \\
 a_g &= - \sum_{m=2}^{N2} m r^{-m-2} \left(\sec \phi \rho_m^m \right) (C_{mm} \sin m\lambda - S_{mm} \cos m\lambda) \\
 &- \sum_{m=1}^{N3} m \sum_{n=m+1}^{N3} r^{-n-2} \left(\sec \phi \rho_n^m \right) (C_{nm} \sin m\lambda - S_{nm} \cos m\lambda) \\
 \\
 a_h &= \sum_{n=2}^{N1} (n+1) \left(J_n r^{-n-2} \right) \rho_n \\
 &- \cos \phi \left[\sum_{m=2}^{N2} (m+1) r^{-m-2} \left(\sec \phi \rho_m^m \right) (C_{mm} \cos m\lambda + S_{mm} \sin m\lambda) \right. \\
 &\quad \left. + \sum_{m=1}^{N3} \sum_{n=m+1}^{N3} (n+1) r^{-n-2} \left(\sec \phi \rho_n^m \right) (C_{nm} \cos m\lambda + S_{nm} \sin m\lambda) \right]
 \end{aligned}$$

where

$$\rho_n = \left[(2n-1) \sin \phi \rho_{n-1} - (n-1) \rho_{n-2} \right] / n \quad n > 0$$

$$\rho_0 = 1$$

$$\rho_1 = \sin \phi$$

$$\rho'_n = \sin \phi \rho'_{n-1} + n \rho_{n-1}$$

$$\rho'_1 = 1$$

and

$$\left(\sec \phi \rho_m^m \right) = (2m - 1) \cos \phi \left(\sec \phi \rho_{m-1}^{m-1} \right)$$

$$\left(\sec \phi \rho_1^1 \right) = 1$$

$$\sec \phi \rho_n^m = \left[(2n - 1) \sin \phi \left(\sec \phi \rho_{n-1}^m \right) - (n + m - 1) \left(\sec \phi \rho_{n-2}^m \right) \right] / (n-m)$$

$$\sec \phi \rho_{m-1}^m = 0$$

and

$$\left(\cos \phi \rho_m^{m'} \right) = -m \sin \phi \left(\sec \phi \rho_m^m \right)$$

$$\left(\cos \phi \rho_n^{m'} \right) = -n \sin \phi \left(\sec \phi \rho_n^m \right) + (n + m) \left(\sec \phi \rho_{n-1}^m \right)$$

These accelerations undergo subsequent coordinate transformations to a system where they are more easily integrated. This is explained in section 3.3 for the case where the moon is the central body.

Integration is accomplished in subroutine TRAJ using a Cowell technique with certain refinements. The process is initiated with a Runge-Kutta starter which sets up the finite differences from which the Cowell integration proceeds. The velocity is summed with an eighth-order Adams-Moulton single sum process. The position is summed from the accelerations with an eight-order Cowell second sum process. Both of these methods use a predictor-corrector formulation. Interpolations for times intermediate between the time steps of the integrations are calculated with a Cowell step.

The time interval between successive steps, i.e., step-size, is automatically controlled to keep seventh-order differences within a certain numerical range. This guarantees a given accuracy but permits the step size to be as large as possible.

3.2 Variational Equations

The normal matrix of the differential correction process (A^TWA matrix) is developed from the A matrix of partial derivative of observations at time t to the various elements in the solution vector. It is necessary to evaluate these partial derivatives. The partial derivatives have two parts, a geometric factor and a time dependent factor. The time dependent factor is derived from a variational equation which describes how a perturbation contributes to the effect of carrying the state vector at epoch to the state vector at some other time.

The general modern approach is to set up the theory as a large matrix operation to systematically represent the influence of all of the partial derivatives. The same matrix formulation also gives insight in their derivation. By examining the full influence of all perturbations on the state vector at epoch, we can derive the matrix variational equations for all partial derivatives.

For the purpose of illustration it is useful to consider a limited case first in which a state vector is defined as

$$\mathbf{x}_t = \begin{bmatrix} \mathbf{r}_t \\ \mathbf{v}_t \end{bmatrix} = \left[x_t, y_t, z_t, \dot{x}_t, \dot{y}_t, \dot{z}_t \right]^T$$

The time derivative of the state vector leads to the equations of motion when physical accelerations are identified with the perturbative potential U .

$$\dot{\mathbf{x}}_t = \begin{bmatrix} \dot{\mathbf{r}}_t \\ \dot{\mathbf{v}}_t \end{bmatrix} = \begin{bmatrix} \mathbf{v}_t \\ \frac{\partial U}{\partial \mathbf{r}_t} \end{bmatrix} = f(\mathbf{x}_t, t)$$

where $\partial U / \partial \mathbf{r}_t$ are the nonzero partial derivatives of U with respect to the components of \mathbf{x}_t . Integration of the equations of motion from the initial conditions defined as the state vector at epoch leads to the spacecraft trajectory. Differentiation of the equations of motion with respect to the state vector at epoch leads to the variational equations:

$$\frac{\partial \dot{\mathbf{x}}_t}{\partial \mathbf{x}_0} = \frac{\partial f}{\partial \mathbf{x}_t} \cdot \frac{\partial \mathbf{x}_t}{\partial \mathbf{x}_0}$$

which may be written (under proper assumptions)

$$\frac{d}{dt} \left(\frac{\partial \mathbf{x}_t}{\partial \mathbf{x}_0} \right) = \frac{\partial f}{\partial \mathbf{x}_t} \cdot \frac{\partial \mathbf{x}_t}{\partial \mathbf{x}_0}$$

A simple change in notation

$$X = \frac{\partial x_t}{\partial x_0}$$

$$A = \frac{\partial f}{\partial x_t} = \begin{bmatrix} 0_3 & I_3 \\ \frac{\partial^2 U}{\partial r_t^2} & 0_3 \end{bmatrix}$$

$$\dot{X} = AX, \quad X(t_0) = I_6$$

This equation represents a set of 36 linear differential equations which are usually called the variational equations. The solution to this set of equations is the matrix X which is called either the fundamental matrix of the set of linear homogeneous differential equations or the state transition matrix which relates the state vector at one time to the state vector at another time

$$x_t = X x_0$$

This development can be generalized to incorporate all of the perturbations so that they too may be simultaneously corrected. The time derivative of the state vector is considered to be a function of the state vector and the gravitational (including earth and sun effects) and radiation pressure perturbations.

$$\dot{x}_t = h(x_t, p)$$

A new, extended state vector z_t incorporating the previous state vector x_t and the coefficients P of the perturbation models is defined. This is the dynamic portion of the solution vector.

*To develop the variational equations for the gravitational potential constants, first write the equations of motion of a point mass under the effects of gravity,

$$\frac{d^2}{dt^2} x_i = \frac{\partial}{\partial x_i} \left(-\frac{\mu}{r} + U \right), \quad i = 1, 2, 3$$

where μ is the gravitational constant, $r^2 = x_1^2 + x_2^2 + x_3^2$, and U is the "perturbation potential," i.e., the difference between the actual potential of the body and that of an equal mass concentrated at the center of gravity. Differentiating the first term gives

$$\frac{d^2}{dt^2} x_i = -\mu \frac{x_i}{r^3} - \frac{\partial U}{\partial x_i}, \quad i = 1, 2, 3 \quad (1)$$

or, with the notation

$$\mu a_i = -\frac{\partial U}{\partial x_i} \quad i = 1, 2, 3 \quad (2)$$

$$\frac{1}{\mu} \frac{d^2}{dt^2} x_i = -\frac{x_i}{r^3} + a_i \quad i = 1, 2, 3$$

The x_1, x_2, x_3 represents the inertial, orthogonal, selenocentric coordinate system. The x_1 axis is directed toward the vernal equinox and the x_3 axis is normal to the earth's equatorial plane.

* The remainder of this section is the work of O. K. Smith.

The potential U can be written as

$$U = \mu \left\{ \sum_{n=2}^{\infty} \gamma^{-n-1} \left[J_n P_n(\sin \phi) - \sum_{n=1}^{\infty} (C_{nm} \cos m\lambda + S_{nm} \sin m\lambda) P_n^m(\sin \phi) \right] \right\} \quad (3)$$

where ϕ is the latitude and λ is the longitude.

Variational equations may be derived by differentiation. If p represents one of the six components of the state vector, or orbital elements, etc., then by differentiating equation 1:

$$\frac{d^2}{dt^2} \left(\frac{\partial x_i}{\partial p} \right) = \sum_{j=1}^3 v_{ij}(t) \left(\frac{\partial x_j}{\partial p} \right) \quad (4)$$

where

$$v_{ij}(t) = -\mu \left[\frac{\partial}{\partial x_j} \left(\frac{x_i}{r^3} \right) + \frac{1}{\mu} \frac{\partial^2 U}{\partial x_i \partial x_j} \right]$$

with the time dependence of v_{ij} arising through its dependence on the solution $x_1(t)$, $x_2(t)$, $x_3(t)$ of equation 1. Initial conditions for equation 4 depend on the choice of the parameters p .

The equations of variation for the gravitational constant are, from equations 1 and 2,

$$\frac{d^2}{dt^2} \left(\frac{\partial x_i}{\partial \mu} \right) = \sum_{j=1}^3 v_{ij}(t) \left(\frac{\partial x_j}{\partial \mu} \right) - \left(\frac{x_i}{r^3} - a_i \right); \quad i = 1, 2, 3 \quad (5)$$

with zero initial conditions, while for any other coefficient c in the potential

they are

$$\frac{d^2}{dt^2} \left(\frac{\partial x_i}{\partial c} \right) = \sum_{j=1}^3 V_{ij}(t) \left(\frac{\partial x_j}{\partial c} \right) + \left(\frac{\partial a_i}{\partial c} \right) \quad (6)$$

again with zero conditions.

Thus, all of the necessary equations are linear with the same coefficient matrix V_{ij} , and differ only in the inhomogeneous terms (equations 5 and 6). Except for the $\partial a_i / \partial c$ terms, all of the terms for these equations are already being computed in the variational equations for the initial conditions. The $\partial a_i / \partial c$ partials are calculated most easily in a local (f, g, h) system (see section 3.1) and then rotated back to the x_1, x_2, x_3 inertial system for integration. It is convenient to evaluate the $\partial a_i / \partial c$ at the same time the recursive potential is computed, since there are several quantities which are needed in both computations (e.g., the Legendre polynomials, powers of the central body radius vector, etc.); hence, they are included in the GPERT output. The $\partial a_i / \partial c$ partials are as follows:

Jn

$$\frac{\partial a_f}{\partial J_n} = r^{-(n-2)} \cos \phi$$

$$\frac{\partial a_g}{\partial J_n} = 0$$

$$\frac{\partial a_h}{\partial J_n} = r^{-(n+2)} (n+1) P_n$$

The argument of the Legendre polynomial is understood to be $(\sin \phi)$.

C_{mm}, S_{mm} (sectoral)

$$\frac{\partial a_f}{\partial C_{mm}} = \cos m \lambda m \sin \phi r^{-(m+2)} (\sec \phi P_m^m)$$

$$\frac{\partial a_f}{\partial S_{mm}} = \sin m \lambda m \sin \phi r^{-(m+2)} (\sec \phi P_m^m)$$

$$\frac{\partial a_g}{\partial C_{mm}} = - \sin m \lambda m r^{-(m+2)} (\sec \phi P_m^m)$$

$$\frac{\partial a_g}{\partial S_{mm}} = \cos m \lambda m r^{-(m+2)} (\sec \phi P_m^m)$$

$$\frac{\partial a_h}{\partial C_{mm}} = - \cos m \lambda (m+1) r^{-(m+2)} \cos \phi (\sec \phi P_m^m)$$

$$\frac{\partial a_h}{\partial S_{mm}} = - \sin m \lambda (m+1) r^{-(m+2)} \cos \phi (\sec \phi P_m^m)$$

$\frac{C_{nm}, S_{nm}}{m < n}$, (tesseral)

$$\frac{\partial a_f}{\partial C_{nm}} = - \cos m \lambda r^{-(n+2)} (\cos \phi P_n^{m'})$$

$$\frac{\partial a_f}{\partial S_{nm}} = - \sin m \lambda r^{-(n+2)} (\cos \phi P_n^m)$$

$$\frac{\partial a_g}{\partial C_{nm}} = - \sin m \lambda r^{-(n+2)} (\sec \phi P_n^m)$$

$$\frac{\partial a_g}{\partial S_{nm}} = \cos m \lambda r^{-(n+2)} (\sec \phi P_n^m)$$

$$\frac{\partial a_h}{\partial C_{nm}} = - \cos m \lambda (n+1) r^{-(n+2)} \cos \phi (\sec \phi P_n^m)$$

$$\frac{\partial a_h}{\partial S_{nm}} = - \sin m \lambda (n+1) r^{-(n+2)} \cos \phi (\sec \phi P_n^m)$$

with

$$\cos \phi P_n^{m'} = -n \sin \phi (\sec \phi P_n^m) + (n+m) (\sec \phi P_{n-1}^m)$$

The partials are now rotated back to the (x_1, x_2, x_3) system before being added to equation 6.

$$\begin{bmatrix} \frac{\partial a_1}{\partial c} \\ \frac{\partial a_2}{\partial c} \\ \frac{\partial a_3}{\partial c} \end{bmatrix} = \begin{bmatrix} \cos \alpha \sin \phi & -\sin \alpha & \cos \phi \cos \alpha \\ \sin \alpha \sin \phi & \cos \alpha & \cos \phi \sin \alpha \\ -\cos \phi & 0 & \sin \phi \end{bmatrix} \begin{bmatrix} \frac{\partial a_f}{\partial c} \\ \frac{\partial a_g}{\partial c} \\ \frac{\partial a_h}{\partial c} \end{bmatrix}$$

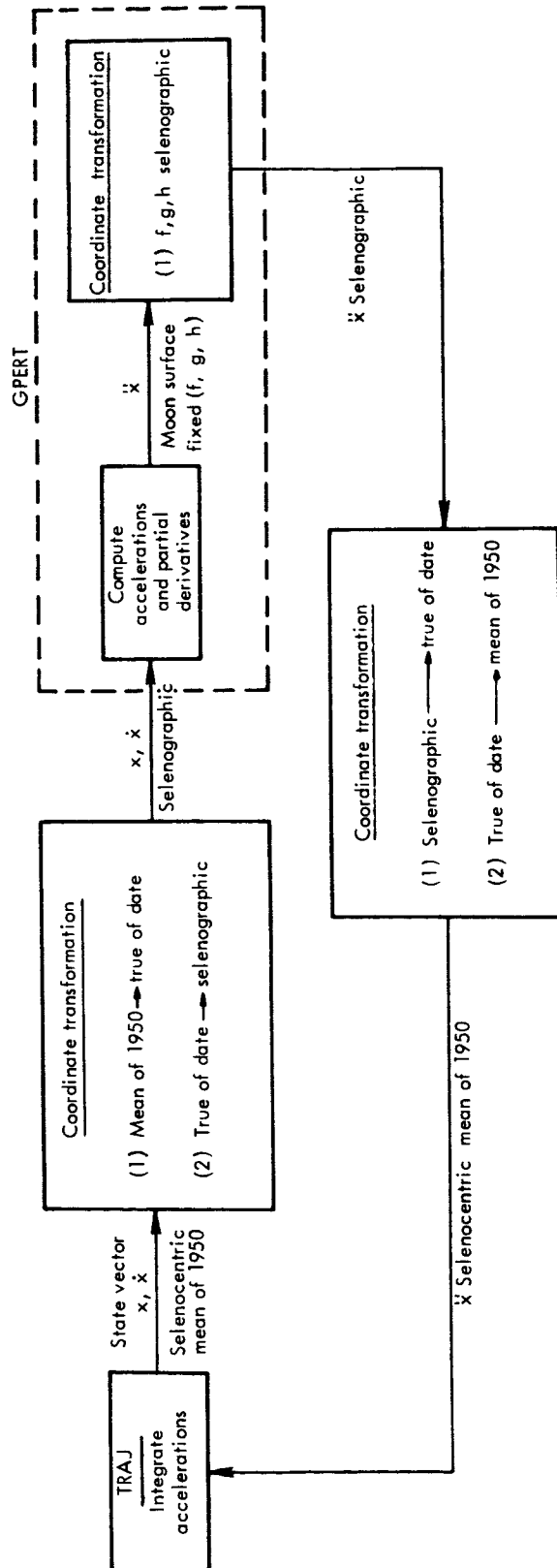
For lunar trajectories, the (x_1, x_2, x_3) system is selenographic so that ϕ and λ are the selenographic latitude and longitude.

3.3 Transformations from GPERT to TRAJ

The block diagram of figure 1 illustrates the coordinate transformations necessary to generate the lunar trajectory. The same loop applies to the integration of the variational equations.

The TRAJ subroutine integrates the actual trajectory and variational equations. This is done in an inertial (x_1, x_2, x_3) system, mean of 1950; i.e., the x_1 axis is directed toward the mean equator and equinox of 1950 (normally abbreviated "mean of 1950"). This frame was chosen because the ephemeris tapes are written in mean of 1950.

Coming out of TRAJ, we have a state vector (position, velocity) and partial derivatives in selenocentric mean of 1950. The state vector is then transformed to selenographic and input to GPERT. Since GPERT computes the perturbative accelerations for the next step of the integration, it must know the vehicle position with respect to the asymmetrical mass distribution of the moon. After computation, the accelerations are rotated to the mean-of-1950 system. TRAJ can then accept the accelerations in mean of 1950 and provide by integration the mean-of-1950 state vector for the next iteration.



NOTE:
 Partial derivatives undergo the same
 sequence of transformations as the
 state vector.

Figure 1.- Coordinate Transformations in the Integration
 of the Perturbative Accelerations

4. TEST CASES

A total of four test cases were designed to demonstrate the capability of the AT85 orbit determination program in solving for lunar potential constants. Simulated observations in range and range rate were generated from the Deep Space Network (DSN) tracking stations at Woomera, Goldstone, and Madrid. The trajectory used to generate these observations used Goudas' lunar constants. The initial estimates of these constants were then perturbed, and the program was used in an attempt to recover the nominal values.

4.1 Lunar Potential Model

The following constants (except for μ) and their uncertainties were taken from reference 1. The C and S notation conforms with the expansion of equation 1, in section 3.1.

TABLE I.—LUNAR CONSTANTS

Lunar constant	Value x 10 ⁻⁴	1 σ Uncertainty x 10 ⁻⁴	Units
μ	.68023264	.000042	(earth radii) ³ /(min) ²
J ₂	2.048	0.1	none
J ₃	0.863	.099	—
J ₄	-2.628	.556	—
S ₃₁	.296	.099	—
S ₄₁	.403	.230	—
S ₃₃	.0067	.0105	—
S ₄₃	.0075	.0025	—
C ₂₂	.23	0.1	—
C ₃₂	-.069	.062	—
C ₄₂	-.0825	.0422	—
C ₄₄	.0211	.0075	—

The above uncertainties were used to perturb the original trajectory in the curve fit. The value of the perturbation was three times the one-sigma uncertainty shown above.

4.2 Description of Test Case

The following is a summary of each test case and the results obtained. Two different trajectories were used. Their characteristics are tabulated below.

TABLE II.- TRAJECTORY DESCRIPTION

Description	Trajectory 01	Trajectory 02
Injection time (GMT)	June 17, 1966 13 ^h 5 ^m 13.92 ^s	June 27, 1966 4 ^h 0 ^m 48. ^s
Selenocentric coordinates		
x (km)	950.17148	1626.7478
y	-2400.6717	1082.9332
z	-364.25808	365.48493
\dot{x} (km/sec)	1.0958210	-.97861241
\dot{y}	.84073599	1.1517809
\dot{z}	.28029238	.94300413
Selenographic elements		
a (km)	2763.0875	2788.0
e	.29857857	.2869
i (deg)	12.5	15.0
Ω (deg)	307.71	25.47
ω (deg)	186.34	-12.46
M (deg)	297.675	0.

Three radar stations were used: Goldstone, Woomera, and Madrid. Range and range-rate measurements were taken at a rate of one set per minute from each station. The simulated observations were generated for both trajectory 01 and trajectory 02. The injection vector appears in table II and the lunar constants in table I. Uncorrelated gaussian random noise was added to the range and range-rate measurements with standard deviations of 15 meters in range and .02 meter/sec in range rate. In addition, a positive range bias of 20 meters was added to all range observations. The moon was not considered transparent. A separate program was used to remove simulated observations when occulted by the moon. Table III summarizes the station characteristics.

TABLE III.- RADAR STATIONS

Station	Latitude °	Longitude °E	Elevation (m)
Goldstone	35.206	243.150	1004.
Woomera	-31.210	136.885	156.
Madrid	40.437	-3.765	800.

4.3 Running Time

The following formula will approximate the 7090 running time.

$$\text{Time (min)} = 5 + 2.5 \times 10^{-4} (\# \text{ observations}) (\# \text{ iterations}) (\# \text{ variables})$$

The running time is proportional to the number of observations, iterations, and variables with an additive constant of 5 minutes to allow for reading the program plus the input instruction.

Case A

Description: Trajectory 01 was used. Twelve variables were perturbed and the solution vector contained the same 12 variables. A total of 1450 range and 1450 range-rate measurements was included. The data rate is one observation per minute when the station is visible. The data arc covers 9 hours of tracking after epoch. Epoch was taken at June 17, 1966 - $13^{\text{h}}/5^{\text{m}}/13.92^{\text{s}}$ GMT, the injection time of table II.

Results: Results are tabulated on the following page. The uncertainty column in the table is the 1σ error associated with each unknown. Because of the statistical nature of the observations, absolute certainty is impossible. The fourth column indicates the amount by which the arrived-at value exceeds the nominal value of table I.

TABLE IV. - RESULTS CASE A

Lunar constant	Nominal value x 10 ⁻⁴	Regressed value x 10 ⁻⁴	1σ uncertainty x 10 ⁻⁴	Error in estimate, σ
μ	.68023264	.68019937	.00000734	4.53
J ₂	2.048	3.447	.323	4.33
J ₃	.863	1.065	.147	1.37
J ₄	-2.628	-1.616	.276	3.67
S ₃₁	.296	.327	.072	.43
S ₄₁	.403	.407	.017	.24
S ₃₃	.0067	-.0022	.0032	1.41
S ₄₃	.0075	.0181	.0031	3.42
C ₂₂	.23	.17	.016	3.75
C ₃₂	-.069	-.057	.014	.86
C ₄₂	-.0825	-.0978	.0112	1.37
C ₄₄	.0211	.0206	.00057	.88

Number of iterations = 3

Range residuals: mean = 0.52 m; rms = 20.2 m

Range-rate residuals: mean = -.0006 m/s; rms = .021 m/s

Case B

Description: Trajectory 02 was used. As in Case A the same 12 variables were perturbed and solved for. A total of 628 range and 628 range-rate measurements was used. The data span begins at epoch (June 6, 1966 - 4^h/10^m/48^s GMT) and continues for 10 hours. The Madrid station was not visible during this interval.

TABLE V. - RESULTS CASE B

Lunar constant	Nominal value x 10 ⁻⁴	Regressed value x 10 ⁻⁴	1σ uncertainty x 10 ⁻⁴	Error in estimate, σ
μ	.68023264	.68023247	.00000749	.020
J ₂	2.048	2.146	.391	.25
J ₃	.863	.634	.145	1.58
J ₄	-2.628	-2.256	.369	1.01
S ₃₁	.296	.265	.074	.42
S ₄₁	.403	.422	.032	.59
S ₃₃	.0067	.0085	.0045	.40
S ₄₃	.0075	.0024	.0030	1.70
C ₂₂	.23	.18	.013	3.85
C ₃₂	-.069	-.106	.025	1.48
C ₄₂	-.0825	-.1152	.0122	2.68
C ₄₄	.0211	.0200	.00048	2.29

Number of iterations = 3

Range residuals: mean = -.62 m; rms = 20.3 m

Range-rate residuals: mean = -.0007 m/s; rms = .025 m/s

Case C

Description: Trajectory 01 was used. Eleven constants were perturbed and seven solved for. The perturbed values not solved for were S_{33} , S_{43} , C_{42} , and C_{44} . Range and range-rate observations totaled 1550 each at a rate of one per minute. The data arc covered 9-1/2 hours of tracking. Epoch as before was June 6, 1966 - 17^h/13^m/13.92^s GMT.

TABLE VI. - RESULTS CASE C

Lunar constant	Nominal value x 10 ⁻⁴	Regressed value x 10 ⁻⁴	1σ uncertainty x 10 ⁻⁴	Error in estimate, σ
J ₂	2.048	6.113	.274	14.8
J ₃	.863	-2.915	.057	66.3
J ₄	-2.628	3.277	.069	85.6
S ₃₁	.296	-1.076	.018	76.2
S ₄₁	.403	.0078	.0011	359.3
C ₂₂	.23	-.164	.004	98.5
C ₃₂	-.069	.244	.007	44.7

Number of iterations = 3

Range residuals: mean = 5.18 m; rms = 41.3 m

Range-rate residuals: mean = .0038 m/s; rms = .038 m/s

Case D

Description: Trajectory 01 was used. As in Case C, 11 constants were perturbed, but this time 9 were in the solution. S_{33} and C_{44} were not included in the solution, but were perturbed. A total of 3245 range and range-rate observations were included. This amounts to 20 hours of tracking.

TABLE VII. - RESULTS CASE D

Lunar constant	Nominal value x 10^{-4}	Regressed value x 10^{-4}	1 σ uncertainty x 10^{-4}	Error in estimate, σ
J ₂	2.048	2.691	.021	30.6
J ₃	.863	3.586	.036	75.6
J ₄	-2.628	-4.300	.038	44.0
S ₃₁	.296	1.654	.020	67.9
S ₄₁	.403	.491	.005	17.6
S ₄₃	.0075	.110	.001	102.5
C ₂₂	.23	.421	.008	23.8
C ₃₂	-.069	-.553	.005	96.8
C ₄₂	-.0825	.208	.004	46.7

Number of iterations = 3

Range residuals: mean = 4.02 m; rms = 34.7 m

Range-rate residuals: mean = -.0009 m/s; rms = .034 m/s

5. CONCLUSIONS

The program does indeed provide a corrected state vector of lunar constants within allowable uncertainties whenever each perturbed quantity is included in the state vector. This is the result in Case A and Case B. If the number of perturbed lunar constants exceeds the dimension of the solution vector, the program will not provide a corrected solution within acceptable uncertainties. This is illustrated in Case C and Case D.

6. NEW TECHNOLOGY

This section is included to comply with requirements of the "New Technology clause of the Master Agreement under which this report was prepared. This report describes a study performed using certain orbit determination processes developed by TRW Systems. The most significant new technology resulting from this contract is the recursive formulation for the calculation of partial derivatives.

APPENDIX I

A. INPUT

A typical ESPOD input for the test cases described here might consist of the following:

1. Epoch time.
2. State vector at epoch.
3. The values of the potential constants used in trajectory integration.
4. Flags to determine the quantities included in the potential model.
5. Flags to determine which quantities are to be in the solution vector.
6. Maximum number of iterations.
7. Bounds on the differential correction -- The bounds place an upper limit on the correction on each iteration; a proper choice of bounds will prevent divergence of the solution.
8. Weighting of observation -- The observations are usually weighted by the standard deviation (σ) of the noise. In our case, the weighting corresponded exactly to the noise σ used in generating the data.
9. The sun, earth, and planets may be included as perturbative forces. The test cases contained sun and earth only.
10. Input and output units are usually in ft and ft/sec; however, any other system can be used. This is controlled by two input cards.
11. The final corrected trajectory may be called for at any desired sequence of time points.

B. OUTPUT

A typical output print will furnish the following information :

1. Card image of all input statements.
2. Station locations.
3. Chronological listing of all radar observations, i.e., time, range, azimuth, elevation, range rate, etc.
4. Listing of program constants, potential constants, radius of earth, etc.
5. Residuals, listed chronologically or by station, at each iteration.
6. The mean and rms of all residuals at a particular station.
7. The differential correction for the particular iteration, with the old and new value of the solution vector, the bounds, and the sigma involved for variables in the solution vector... sigma is the square root of the diagonal element of the covariance matrix, $(A^TWA)^{-1}$.
8. The corrected state vector at epoch in true of date, ADBARV, and Cartesian coordinates.
9. Statements as to whether or not solution is converging or affected by the bounds.
10. The weighted rms of the residuals for the current iteration, the predicted for the next iteration, and the best rms up to the current iteration.
11. The covariance matrix of the solution and its associated correlation matrix.
12. A printout of the final corrected trajectory.

APPENDIX II

CORRELATION MATRICES

The correlation matrices were obtained from the covariance matrix $(A^TWA)^{-1}$ by dividing the (i,j) element by $\sigma_i \sigma_j$. Rows and columns containing zeros indicate that this variable was ignored in all final computations. The correlation matrices for the four test cases are given on the following pages.

CASE A

CORRELATION MATRIX

	1	2	3	4	5	6	7	8
J2	1.000000000							
J3	0.336300075	1.000000000						
J4	0.905514680	-0.073947236	1.000000000					
C31	0.	0.	0.	1.000000000				
S31	0.327199109	0.967889823	-0.097320840	-0.	1.000000000			
C41	0.	0.	0.	-0.	0.	1.000000000		
S41	0.316333182	0.58446839	0.195090972	-0.	0.374756984	0.	1.000000000	
C22	0.212678649	0.780726783	-0.139125012	-0.	0.875760823	0.	0.251503594	1.000000000
S22	0.	0.	0.	0.	-0.	-0.	-0.	-0.
C32	0.090075076	-0.783563264	0.183527276	0.	-0.723350354	-0.	-0.678746887	-0.704503246
S32	0.	0.	0.	0.	-0.	-0.	-0.	-0.
C42	0.195250459	0.812687725	-0.186746709	-0.	0.919432417	0.	0.119735770	0.928445935
S42	0.	0.	0.	0.	-0.	-0.	-0.	-0.
C33	0.378317133	0.671743855	0.163676724	-0.	-0.	-0.	-0.	-0.
S33	0.	0.	0.	0.	0.615891524	0.	0.613131665	0.501990505
C43	0.	0.	0.	-0.	0.	0.	0.	0.
S43	0.652975157	-0.488212757	-0.492393218	0.	-0.450530678	-0.	-0.572892703	-0.372128725
C44	0.469385222	0.082513258	-0.558391154	0.	0.195749462	-0.	-0.304511011	0.280069418
S44	0.	0.	0.	-0.	0.	0.	0.	0.
MU	0.982124180	-0.471042573	-0.825630493	0.	-0.460081480	-0.	-0.338644080	-0.313205823

	9	10	11	12	13	14	15	16
S22	1.000000000							
C32	0.	1.000000000						
S32	0.	0.	1.000000000					
C42	0.	-0.696570501	0.	1.000000000				
S42	0.	0.	0.	-0.	1.000000000			
C33	0.	0.	0.	0.	0.	1.000000000		
S33	0.	-0.719325073	-0.	0.542733297	-0.	-0.	1.000000000	
C43	0.	0.	-0.	0.	-0.	-0.	0.	1.000000000
S43	0.	0.182820201	0.	-0.207911797	0.	0.	-0.474053212	-0.
C44	0.	-0.329033636	0.	0.465842120	0.	0.	0.134031370	-0.
S44	0.	0.	-0.	0.	-0.	-0.	0.	0.
MU	0.	0.193187751	0.	-0.319943741	0.	0.	-0.469728336	-0.

17 18 19 20

S43	1.000000000							
C44	0.526642881	1.000000000						
S44	0.	0.	1.000000000					
MU	0.642404646	0.428196646	-0.	1.000000000				

CASE C

CORRELATION MATRIX

	1	2	3	4	5	6	7	8
J2 1	1.00000000							
J3 2	-0.526455601	1.00000000						
J4 3	0.929712219	-0.784430422	1.00000000					
C31 4	0.	0.	0.	1.00000000				
S31 5	-0.706596151	0.973058778	-0.902604640	-0.	1.00000000			
C41 6	0.	0.	0.	0.	0.	1.00000000		
S41 7	0.337579533	0.591322668	0.007335387	0.	0.405277811	0.	1.00000000	
C22 8	0.720052347	-0.345950216	0.68981630	-0.	-0.501820236	-0.	0.375300430	1.00000000
S22 9	0.	0.	0.	0.	0.	0.	0.	-0.
C32 0	-0.486714296	-0.461265475	-0.177798204	0.	-0.255487874	0.	-0.971050180	-0.502612382

S3211 -0. 0. -0. -0. 0. -0. -0. 0. 0.

9 10 11

S22 9 1.00000000
 C3210 0. 1.00000000
 S3211 -0. -0. 1.00000000

CASE D

CORRELATION MATRIX

	1	2	3	4	5	6	7	8
J2	1.000000000							
J3	-0.221046910	1.000000000						
J4	0.627613939	-0.844403818	1.000000000					
C31	0.	0.	0.	1.000000000				
S31	-0.206733242	0.943515323	-0.884612188	0.	1.000000000			
C41	0.	0.	0.	0.	0.	1.000000000		
S41	0.080554917	0.709335916	-0.307529844	0.	0.461466134	0.	1.000000000	
C22	-0.305188663	0.916945554	-0.885282941	0.	0.959520295	0.	0.480635777	1.000000000
S22	0.	0.	0.	-0.	-0.	-0.	-0.	-0.
C32	0.553434245	-0.823718108	0.760628499	0.	-0.681398287	0.	-0.721875519	-0.751035891
S32	0.	0.	0.	0.	0.	0.	0.	0.
C42	-0.446891539	0.831816673	-0.935454056	0.	0.938689783	0.	0.249875404	0.940897092
S42	0.	0.	0.	0.	0.	0.	0.	0.
C43	0.	0.	0.	-0.	-0.	-0.	-0.	-0.
S43	-0.787776887	-0.299924016	-0.037345819	-0.	-0.396713756	-0.	-0.195001401	-0.279177807
S22	9	10	11	12	13	14	15	
C32	1.000000000							
S32	0.	1.000000000						
C42	-0.692842089	0.	1.000000000					
S42	0.	0.	0.	1.000000000				
C43	0.	0.	-0.	-0.	1.000000000			
S43	-0.229114361	-0.	-0.151862332	-0.	0.	1.000000000		

REFERENCES

1. Gondas, C. L. : Lunar Potential Constants. Icarus, Vol. 3, 1964, p. 408.
2. Michael and Tolson : The Lunar Orbiter Selenodesy Experiment. Paper presented at the Second International Symposium on "The Use of Artificial Satellites for Geodesy," Athens, Greece, April 1965.
3. Smith, O. K. : The Recursive Computation of Earth Oblateness Perturbations. Memo 9851-238, TRW Systems, TRW Inc., Nov. 20, 1965.
4. Mercer, R.J.: Calculation of Gravitational Force Components. AIAA Journal, vol. 2, June 1964, p. 1166.